Electrochimica Acta 441 (2023) 141766

Contents lists available at ScienceDirect

Electrochimica Acta

journal homepage: www.journals.elsevier.com/electrochimica-acta

Influence of natural convection on the electrodeposition of copper nanowires in anodic aluminium oxide templates

I.A. Kalinin [a,b], A.D. Davydov [c], A.P. Leontiev [b], K.S. Napolskii [b,d], A. Sobolev [e], M. Shatalov [e], M. Zinigrad [e], D. Bograchev [a,*]

[a] Department of Chemical Sciences, Ariel University, Ariel 40700, Israel
[b] Department of Materials Science, Lomonosov Moscow State University, Moscow 119991, Russia
[c] Frumkin Institute of Physical Chemistry and Electrochemistry, Russian Academy of Sciences, Moscow 119071, Russia
[d] Department of Chemistry, Lomonosov Moscow State University, Moscow 119991, Russia
[e] Department of Chemical Engineering, Ariel University, Ariel 40700, Israel

ARTICLE INFO

Keywords:
Nanowires
Templated electrodeposition
Anodic aluminium oxide
Natural convection
Mathematical modeling

ABSTRACT

Templated electrodeposition is a versatile method for preparing metal nanostructures. Among the various parameters of this process, the effect of convection on the deposition process is less explored. The present work is devoted to the experimental and theoretical study of the influence of natural convection near nanoporous anodic aluminium oxide templates on the deposition of nanowires. Electrochemical deposition of copper nanowires was carried out with vertical templates parallel to the gravitational acceleration at various overpotentials. A model of nanowire electrodeposition was developed based on the Navier–Stokes and diffusion equations. The length profiles of the nanowires, experimentally measured using scanning electron microscopy, were compared with the results of the numerical simulation. The simulation results were also compared with current-time transients recorded during metal electrodeposition into nanopores. In addition, an analytical expression has been proposed to describe the evolution of the deposition current density into nanopores under natural convection conditions.

1. Introduction

Templated electrodeposition of metals, alloys, and semiconductors in deep pores of nanosized diameter finds various applications in the manufacture of nanodevices in areas such as optoelectronics, high-density magnetic recording, and sensorics. The nanowires obtained by this method from nickel, copper, and catalytically active metals of the platinum group can be used as interconnectors and building blocks for nanodevices, drug delivery and as (electro)catalysts of chemical and electrochemical reactions, including those in modern types of electrochemical power sources [1–3].

There are many experimental studies [4–7] and a number of theoretical works [8–18] devoted to the electrodeposition of nanowires in porous anodic aluminium oxide (AAO). In these studies, the questions of the rate and simultaneity of pore filling and the dependence of these characteristics on the overpotential, composition, concentration, and temperature of the electrolyte were studied.

Insufficient attention is given to the influence of convection of the solution, and only in a few experimental works have pore filling processes been carried out in stirred solutions [4,19,20]. Moreover, a strong influence of electrolyte agitation on the rate of the electrodeposition process was noted in [20]. The role of forced convection is specifically studied in the author's theoretical work [8]. The external hydrodynamic flow can have a significant effect on the uniformity of the deposition of nanowires into the pores of the template as the forced convection affects the thickness of the diffusion layer.

In the process of electrodeposition of metals, a concentration gradient often occurs between the bulk of the solution and the region near the cathode surface. This should cause natural convection. Natural convection may occur in the absence of forced convection in electrochemical systems [21–24]. Indeed, in experiments with the anode located above the cathode (above the template surface), the filling of pores occurred somewhat faster than with reversed electrode positioning [25].

Natural convection cannot influence the hydrodynamic movement in the nanopore depth, since the diameter of the nanopores is much smaller than any reasonable thickness of Prandtl's layer, i.e., the viscous forces will not allow movement associated with natural convection to be

* Corresponding author.
E-mail address: daniilb@ariel.ac.il (D. Bograchev).

https://doi.org/10.1016/j.electacta.2022.141766
Received 18 October 2022; Received in revised form 23 December 2022; Accepted 24 December 2022
Available online 25 December 2022

developed in the pore depth. However, the hydrodynamic flow associated with electrophoretic effects can play a significant role in the mass transfer within the nanopores [26].

Natural convection plays an important role in classical electrochemical systems since aqueous electrolytes are characterised by large Schmidt numbers (ratio of kinematic viscosity to diffusion coefficient $Sc = \nu/D$ [27]) and strong dependencies of density on solution concentration $\frac{\partial\rho}{\partial c}$ [28]. Therefore, in nanoporous templates, the free convection can similarly organize mixing in a free electrolyte near the template surface. This is a factor that determines the concentration at the mouth of the pores and, accordingly, affects the kinetics of electrodeposition.

Due to this effect, it is possible to estimate the intensity of convection in a system with a template, similar to the usual case of natural convection near a vertical electrode, by using the concentration Rayleigh number:

$$Ra = \frac{g c_0 \frac{\partial\rho}{\partial c} H^3}{\rho D \nu}, \quad (1)$$

where g is the gravity acceleration, c_0 is the bulk concentration, and H is the lateral length of the deposition area.

As can be seen in Eq. (1), even for a system of one centimetre, the Rayleigh number can reach tens of millions, which can lead to turbulence of the naturally convective motion, or at least to its non-stationarity. Even for the system considered in this paper (see Table 1), the estimation of the Rayleigh number gives values of approximately one hundred thousand, which corresponds to the developed natural convection case.

In this work, we aim to consider the effect of natural convection on the global inhomogeneity of electrodeposition into AAO nanopores. Therefore, we carry out experiments on the electrochemical deposition of copper nanowires into the pores of a vertically aligned AAO template, study the effect of natural convection using scanning electron microscopy (SEM), and develop a theoretical model of electrodeposition taking into account natural convective electrolyte motion near the porous template.

2. Experimental

2.1. Fabrication of the AAO templates

Aluminium foil (99.99%, GOST 25905-83, thickness of 100 μm) was used as the starting material for preparing AAO templates. The foil was electrochemically polished to a mirror finish in an intensively stirred solution containing 1.85 M CrO_3 (99.7%, Chimmed) and 13 M H_3PO_4 (85%, Chimmed) at 80°C. The process was performed in pulsed mode: 40 impulses with an anodic current density of 400 mA/cm^2 were applied. The duration of each impulse was 3 seconds and the interval between them was 40 seconds.

Two-step anodization [29] was used to obtain AAO films with an ordered porous structure on the top and bottom surfaces of the template. Anodization was carried out in a two-electrode electrochemical cell in 0.3 M oxalic acid (99.5%, Chimmed) at 0°C with intensive stirring. A constant voltage of 40 V was applied using a N8741A DC power supply (Agilent). The thickness of the AAO films was controlled coulometrically using a charge density-to-thickness ratio of 2.08 C·cm^{-2}·μm^{-1}. The thickness of the AAO film after the first anodization was 20 μm. Then, the AAO film was selectively dissolved in 0.5 M H_3PO_4 and 0.2 M CrO_3 solution at 70°C for 15 min. The obtained Al foil with an ordered array of nanoconcaves on the surface was repeatedly anodized under the same conditions to obtain a 34-μm-thick AAO film with a highly ordered 2D hexagonal arrangement of pores. After that, aluminium was selectively dissolved in a 4 M solution of Br_2 in CH_3OH. Then, the barrier layer of AAO was chemically etched, and the pores were widened in 0.5 M H_3PO_4 at 60°C for 3 min. Then, AAO films were rinsed in deionized water and isopropanol and dried in a heating chamber at 120°C for 60 min. The morphology of the AAO film is shown in Fig. 1. To make the template suitable for further electrodeposition processing, a 160-nm-thick Cu conductive layer with a 3-nm-thick Cr adhesion layer was formed on the bottom side of the AAO films by magnetron sputtering using a TFSP-842 instrument (VST). Just before sputtering, the AAO films were processed in an EQ-PCE3 vacuum plasma cleaner (MTI Corp.) for 3 min in residual air at 0.18 Torr.

2.2. Electrodeposition of nanowires

Electrodeposition of Cu nanowires was performed in a three-electrode cell from the electrolyte containing 0.1 M $CuSO_4$ and 0.1 M H_2SO_4 (pH = 1.08) in potentiostatic mode using a PARSTAT4000A potentiostat (AMETEK) at room temperature. The cell for electrodeposition is shown schematically in Fig. 2a. The AAO template with a Cu conductive layer was used as a working electrode, whereas Ag|AgCl|3.5 M KCl and a Pt ring served as reference and counter electrodes, respectively. The face of AAO template was in vertical orientation during electrodeposition along the direction of gravity acceleration, see Fig. 2, and the electrolyte was not stirred. The electrodeposition was limited by a total charge of 1 Coulomb and was carried out on a template area of 0.28 cm^2 restricted by the O-ring. To analyse the inhomogeneity of Cu nanowires, the template after electrodeposition was split along the direction of gravity acceleration. The obtained cross-section was analysed, and the length of nanowires at different positions was measured (Fig. 2b). To avoid considering the edge effects related to the presence of the O-ring and cell walls, the points located at least 1 mm from the edge of the deposition area were analysed.

SEM images of the AAO films and Cu nanowires in AAO templates were collected using a MAIA3 scanning electron microscope (TESCAN). Before SEM analysis, a Cr layer with a thickness of 5 nm was sputtered onto the surface of the samples by magnetron sputtering using a Q150T ES coating system (Quorum Technologies). The lengths of the nanowires were determined by statistical analysis of the SEM images using ImageJ software [30].

2.3. Modeling of nanowires deposition under natural convection conditions

In our work, a vertical template was considered with a common diffusion layer of monotonically varying thickness. This orientation of the template has been chosen because the natural convection in such a system is the most studied case.

It is well known that the diffusion layer of natural convection in the

Table 1
Parameters of calculations.

Variable	Value	Source
Diffusion coefficient, D, [cm^2/s]	7.2*10^{-6}	[36]
Mass coefficient, $\frac{\partial\rho}{\partial c}$, [g/mol]	153.8	[28]
Exchange current density, i_0, [A/cm^2]	4.7*10^{-3}	By fitting
Transfer coefficient,α	0.16	By fitting
Lateral length of deposition area, H, [cm]	0.6	Assumed based on the diameter of O-ring
Thickness of the model G, [cm]	0.3	Assumed based on the cell geometry
Kinematic viscosity, ν [cm^2/s]	0.01	Assumed based on viscosity of pure ware under normal condition [21]
Fraction of pores filled with deposited nanowires, γ	0.60 (−0.57 V) 0.67 (−0.37 V) 0.63 (−0.17 V)	Estimated by Faraday's law
Porosity, ε	0.3	According to SEM

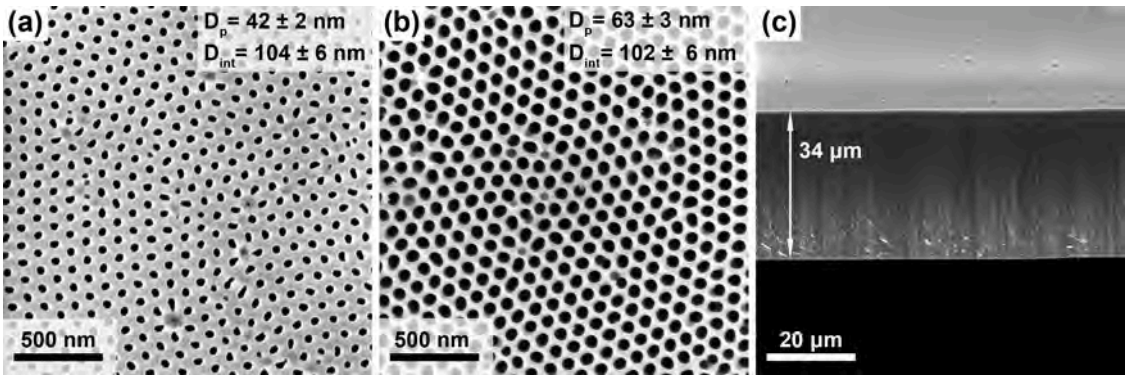

Fig. 1. SEM images of anodic aluminium oxide. (a) Bottom, (b) top, and (c) cross-sectional views of the AAO film obtained by the two-step anodization process after the removal of the barrier layer and the widening of pores by chemical etching, where D_p is the pore diameter and D_{int} is the interpore distance.

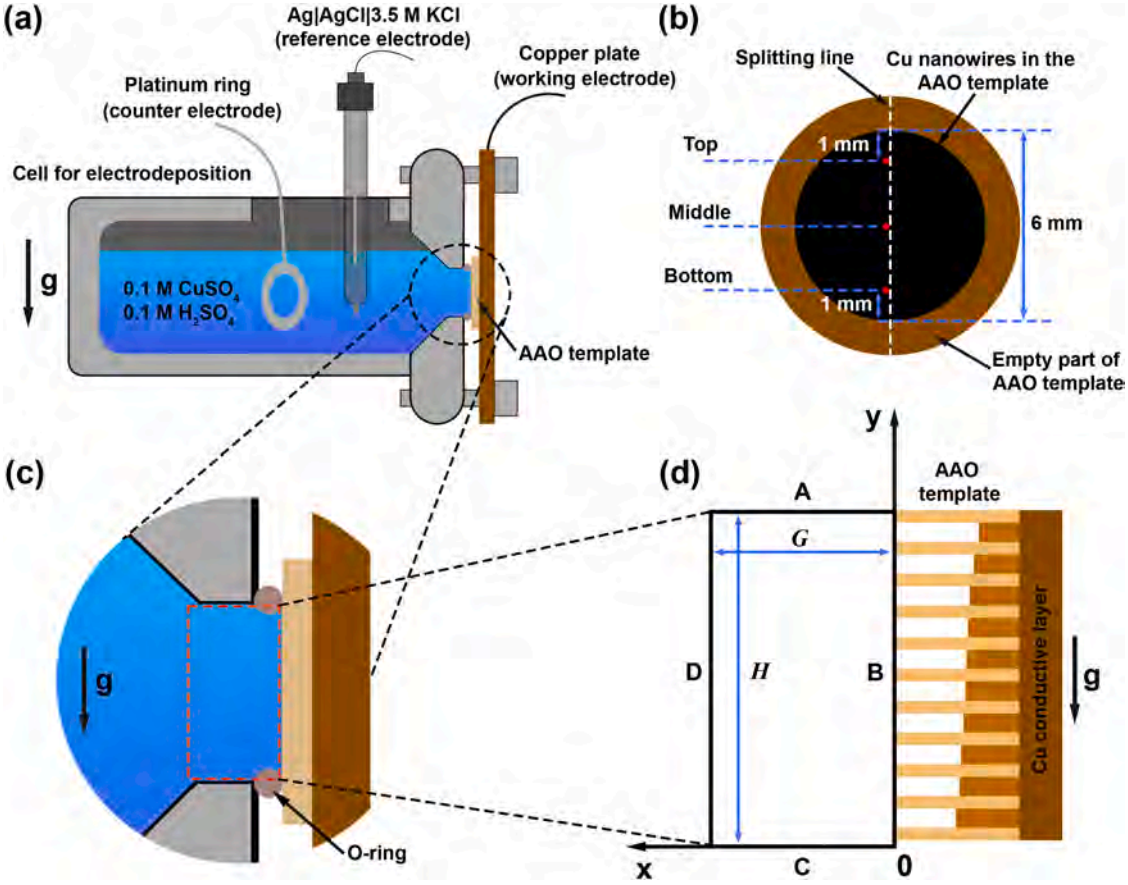

Fig. 2. (a) Schematic view of a three-electrode cell for templated electrodeposition of copper nanowires. (b) Schematic of the sample after electrodeposition of Cu nanowires, illustrating its further splitting along the direction of gravity acceleration and analysis of its various parts. (c) An enlarged view of the cell near the AAO template. The dotted red box indicates the area where the numerical simulation was carried out. (d) Model schematic and coordinate system. Boundaries A and C correspond to the cell walls, boundary B corresponds to the surface of the template, and no-slip conditions are met. At boundary D, the slip condition is satisfied.

electrolyte is also very thin – approximately 100 μm [21]. Therefore, it does not make sense to calculate a large extra volume outside the template area. Therefore, only a narrow cell region next to the template is considered in the model (Fig. 2a–d).

Let us write the equations that describe convection in a non-stationary form, including time derivatives. This is necessary because a system with natural convection can, in principle, be fundamentally non-stationary, especially under high Rayleigh number conditions that can be easily observed in electrochemical systems, as mentioned above. In addition, the diffusion layer grows in the outer region in strong unsteady interactions with the development of hydrodynamic fluid motion:

$$\frac{\partial c}{\partial t} + \mathrm{v}\cdot\nabla c = D\Delta c, \tag{2}$$

$$\frac{\partial \mathrm{v}}{\partial t} + (\mathrm{v}\cdot\nabla)\mathrm{v} = -\frac{\nabla p}{\rho_0} + \nu\Delta\mathrm{v} + \frac{g}{\rho_0}c\frac{\partial \rho}{\partial c}, \tag{3}$$

$$(\nabla\cdot\mathrm{v}) = 0. \tag{4}$$

In Eqs. (2)–(4), the gradients and Laplacians are taken as two-dimensional, and in general, we remain in a two-dimensional system.

Eq. (2) is a non-stationary diffusion equation. Eq. (3) is the Navier–Stokes equation in the Boussinesq approximation, which takes into account the influence of only one component on the change in density. Eq. (4) is the incompressibility condition, where v is the hydrodynamic velocity, ν is the kinematic viscosity, ρ is the pressure, and ρ_0 is the electrolyte density at the volume concentration.

We also accept the no-slip condition on surfaces A, B, and C (Fig. 2d) for the hydrodynamic velocity.

$$\mathrm{v}|_{A,B,C} = 0. \tag{5}$$

On boundary D, the condition that the normal component is equal to zero is accepted:

$$\mathrm{v}_{\mathbf{n}}|_D = 0, \tag{6}$$

where **n** is normal to the boundary.

Hence, we assume that the D boundary is slippery. Such boundary conditions were chosen to minimize the influence of boundaries on the transfer at the template surface.

The boundary condition for the concentration at boundary D is as follows:

$$c|_D = \mathrm{c}_0. \tag{7}$$

At boundaries A and C, the accepted conditions are that the normal component of the diffusion flow is equal to zero (in fact, the total flux is also equal to zero since the velocity on the surface is zero due to the no-slip condition (5)):

$$\left.\frac{\partial c}{\partial \mathbf{n}}\right|_{A,C} = 0. \tag{8}$$

Boundary conditions on the side of the template can be defined following Ref. [8]:

$$D\frac{\partial c}{\partial x}|_B = D\frac{\gamma\varepsilon c|_{x=0}}{L(y,t)+\delta_k}, \tag{9}$$

where ε is the porosity of the template and γ is the pore fraction in which deposition occurs. $\delta_k = \frac{DFz_+c_0}{i_0}\exp\left(\frac{\alpha_c F\eta}{RT}\right)$ is a kinetic length that takes into account the influence of the reaction rate as a certain additional diffusion length, and L is the time-dependent pore depth, which is defined by Faraday's law:

$$\frac{\partial L(y,t)}{\partial t} = -D\frac{M}{\gamma\varepsilon\rho}\frac{\partial c}{\partial x}|_B, \tag{10}$$

with the initial condition for L:

$$L|_{t=0} = d, \tag{11}$$

where d is the initial pore length.

Eq. (9) uses a quasi-stationary approximation inside the template itself [8]. Together with Eq. (10) and the initial condition (11), it allows one to take into consideration the problem of templated electrodeposition as a boundary condition depending on the parameter which is determined from the solution of an ordinary differential equation. For other initial conditions, it was assumed that the hydrodynamic velocity and the pressure are equal to zero at the zero moment of time, and the concentration is equal to the volumetric concentration everywhere.

The measured average deposition current density can be calculated by solving the system of Eqs. (2)–(11) using:

$$\bar{i} = \frac{DFz_+}{S}\int \left.\frac{\partial c}{\partial x}\right|_B ds, \tag{12}$$

where S is the surface area of template.

It is also possible to write out a semiquantitative relation from the expression for the current for a constant thickness of the diffusion layer [8,9] and using half of the maximum diffusion layer thickness obtained by the Galerkin method for natural convection [31]:

$$\bar{i} \approx Dz_+F\frac{\gamma\varepsilon c_0}{\sqrt{\left(\frac{240}{Ra}\right)^{\frac{1}{4}}\left(\frac{H}{2}\gamma\varepsilon+\delta_k+d\right)^2 - 2D\frac{Mc_0}{\rho}t}}, \tag{13}$$

where Ra is determined by Eq. (1).

3. Results and discussion

To determine the range of deposition potentials suitable for the formation of Cu nanowires, cyclic voltammetry measurements were performed. As seen in Fig. 3, at overpotentials below −0.4 V, a plateau corresponding to the diffusion limiting current mode is observed at least to the lowest used overpotential of −0.7 V.

It is worth noting that both reduction of hydrogen and oxygen cannot introduce noticeable impact on the registered current density. Under the experimental conditions, the concentration of dissolved oxygen in the water (2.56×10^{-4} M) [32] is three orders of magnitude lower than the concentrations of Cu^{2+} (0.1 M) used in the work. Moreover, it is known from the literature [33] that the current associated with the reduction of hydrogen grows from 0% to 2.5% in the total current only with an increase of copper electrodeposition overpotential from −0.55 V to −0.7 V. Based on these data, we assume that the current efficiency of Cu electrodeposition is close to 100% and it is possible to ignore the influence of hydrogen evolution on natural convection.

To study different regimes, electrodeposition was carried out at overpotentials of −0.17 V, −0.37 V, and −0.57 V. The lowest overpotential (−0.17 V) and the intermediate overpotential (−0.37 V) correspond to the mixed regime of electrodeposition, whereas the highest overpotential (−0.57 V) corresponds to the diffusion regime. The time dependencies of the current density recorded at various deposition potentials are shown in Fig. 4.

For all overpotentials, the time dependencies of the current density have a characteristic shape for the current transients of the deposition of nanowires. First, the initial values of the current density are at a maximum, then there is a fast decrease in the current, similar to the Cottrell regime [34]. Then, in a relatively short time, the current density reaches a plateau with a slow increase over time. In the absence of forced stirring, this current density behaviour indicates that natural convection is observed in the system, which limits the growth of the diffusion layer. Then, slow growth is observed, which corresponds to a gradual approach of the nanowire deposition front to the template surface and a decrease in the thickness of the total diffusion layer.

As shown in Fig. 4 the currents simulated by the presented model

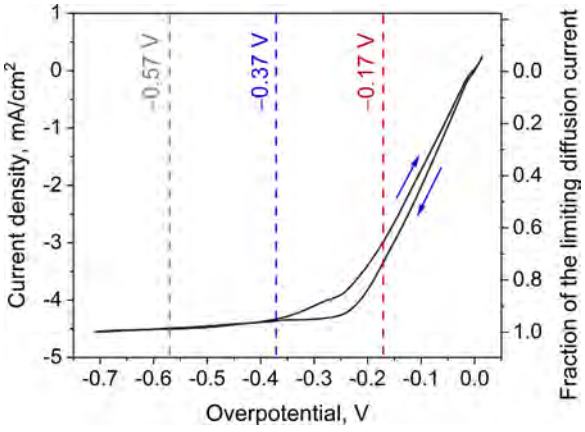

Fig. 3. Cyclic voltammetry of the vertically located porous Cu/AAO electrode in an electrolyte containing 0.1 M $CuSO_4$ and 0.1 M H_2SO_4 recorded at the potential scan rate of 5 mV/s. The dashed lines indicate the potentials used for the potentiostatic electrodeposition of Cu nanowires. The open circuit potential before deposition was 70 mV versus the Ag|AgCl reference electrode.

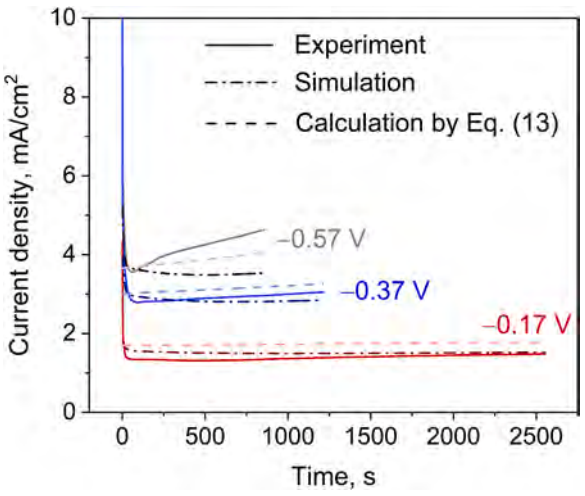

Fig. 4. Time dependencies of current density for the electrodeposition of Cu nanowires into the vertically located AAO templates recorded at various deposition overpotentials: experimental data (solid lines), numerical simulation (dash-dotted lines), and values calculated by Eq. (13) (dashed lines).

(see the system of Eqs. (2)–(12)) agree with the experimental data. On the other hand, the numerical simulation according to the developed model is less in agreement with the experiments than the proposed analytical expression (13) at the highest overpotential.

The fraction of pores where deposition occurred was obtained by estimating from Faraday's law. The obtained value of the exchange current density $i_0 = 4.7 * 10^{-3} A/cm^2$ lies in the range of values mentioned in the reference [35], however, the obtained exchange coefficient has an unusually small value $\alpha = 0.16$.

Fig. 5 shows SEM images of Cu nanowires in different positions in the cross-section of the AAO template. The images show the normalized lengths of nanowires because the maximum length of nanowires (h_{max}) varies slightly in different experiments due to different fractions of pores filled with the metal. For cathodic overpotentials of −0.57 V and −0.37 V, the length of the nanowires increases from the top to the bottom of the AAO template cross-section and reaches the maximum at its lowest point. In the case of a cathodic overpotential of −0.17 V, the length of the nanowires at different positions differs insignificantly, and it is not possible to define the relationship between the geometric position and the length of the nanowires. The collected experimental lengths of the nanowires are presented in Fig. 6a–c; the calculated curves (see Fig. 6d–f) are given for different time points: from 20% to 100% of the deposition time.

The agreement between the calculated and experimental distribu-

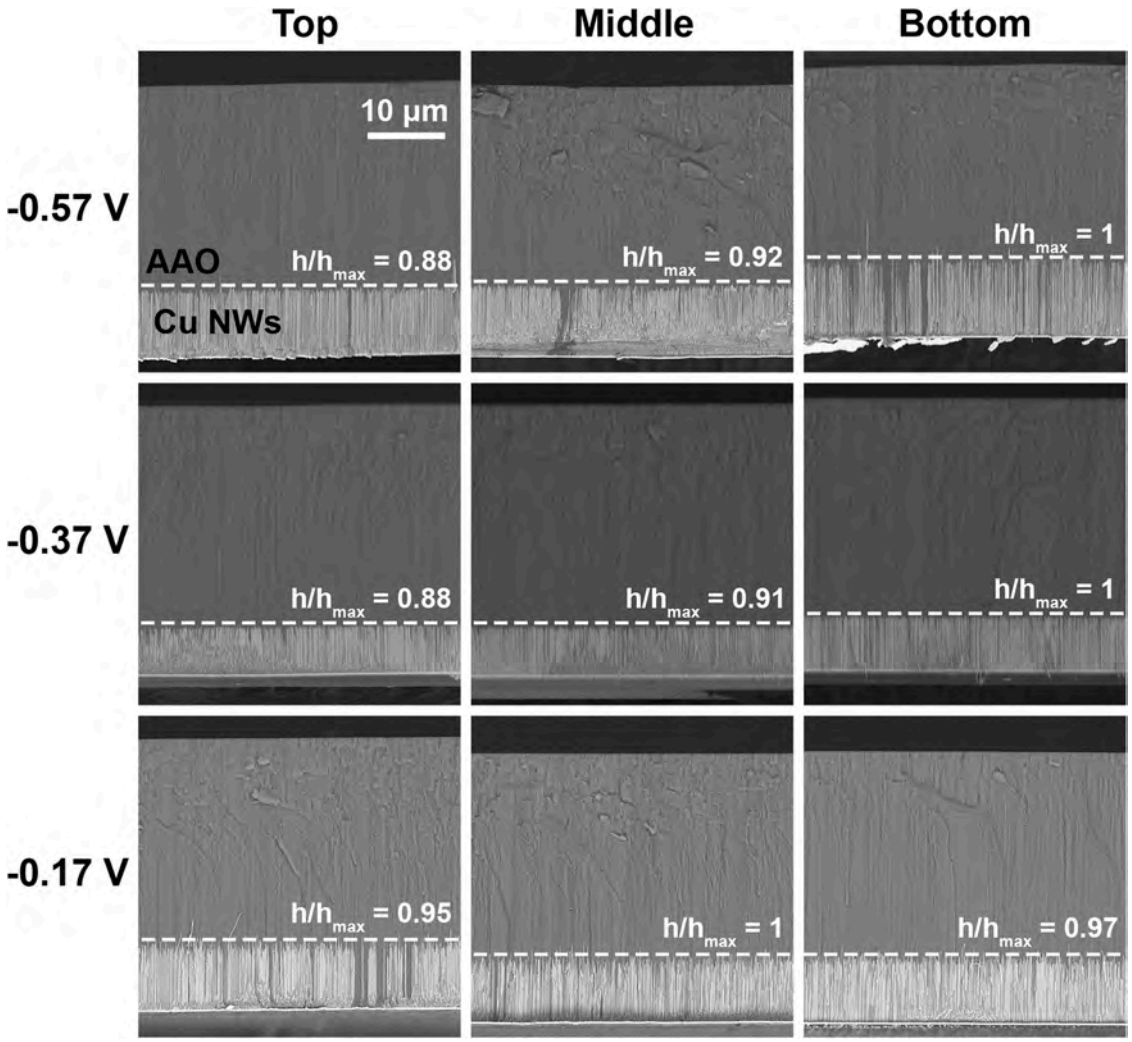

Fig. 5. Cross-sectional SEM images of Cu/AAO nanocomposites in different parts of the template after electrodeposition (top, middle, and bottom) at various deposition overpotentials. The images show the ratio of the length of the Cu nanowires at a given point of the template to the maximum length of the Cu nanowires in the sample under study.

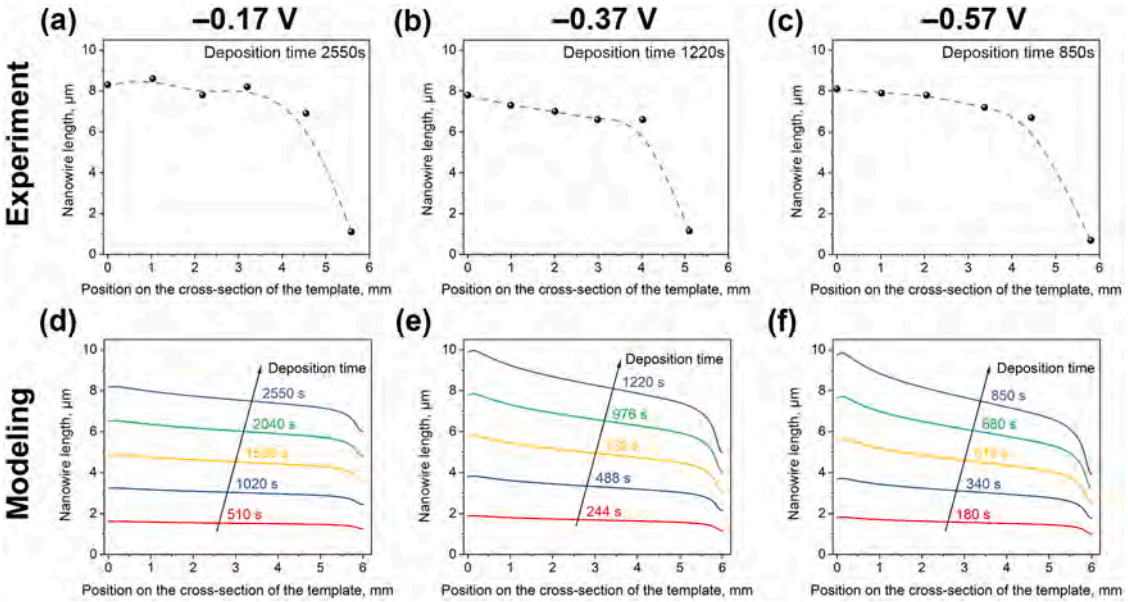

Fig. 6. Experimental distributions of nanowire lengths along the cross-sections of the Cu/AAO nanocomposites obtained at different overpotentials determined according to SEM images (a – c). Simulated distributions of nanowire lengths along the cross-section of the AAO template after various (20%, 40%, 60%, 80%, and 100% of total) deposition times at different overpotentials (d – f). The total charge was 1 Coulomb for all depositions.

tions of the nanowire length is shown. As demonstrated in Fig. 6d–f, the inhomogeneity of the nanowire length in the initial stages of deposition is not as significant. The inhomogeneity develops over time as usual for instability of cathodic deposition [37–39]. At the same time, the resulting inhomogeneity of the lengths of nanowires increases with increasing overpotential; this tendency is observed in the simulation and in the experiment. This can be explained by the fact that when the kinetic length δ_k (see Eq. (9)) at a certain overpotential becomes smaller than the thickness of the inhomogeneous naturally convective diffusion layer, as its effect on deposition weakens.

There is also a drop in nanowire length in the bottom and especially in the top sides of templates, which corresponds to the presence of stagnant zones near the O-ring and walls of the cell. Seemingly, natural convection is suppressed in the corners of the cell, since electrolyte movement does not occur due to the influence of viscosity and the greater thickness of the diffusion layer. It is important to note that there are no such decreases in the current density at the boundaries in the classical problem statement of natural convection near a vertical smooth electrode [21].

Further development of the model leads in several directions. First, it is necessary to create a real 3D model that takes into account the complete geometry of the electrochemical cell. In addition, electrolyte transfer should explicitly take into account the migration term and the transfer of all types of electrolyte ions [40]. The Navier–Stokes equation should also consider changes in the concentration of all types of ions [28]. In addition, it is necessary to take into account the nonlinear dependence of the exchange current on the electrolyte concentration.

4. Conclusions

Experimental and theoretical studies of the effect of natural convection near a vertically located template on the filling of nanopores with metal were carried out. The influence of overpotentials on the nature of the ongoing processes was determined: at overpotentials above –0.4 V, limiting diffusion currents of electrodeposition were observed; at overpotentials from –0.37 V to –0.1 V, both diffusion and kinetic limitations appeared, i.e., the process proceeded in a mixed mode. The dependence of the deposition currents on time was measured, which made it possible to determine the exchange current $i_0 = 4.7 * 10^{-3} A$ / cm^2 and the transfer coefficient $\alpha = 0.16$ of the deposition of Cu nanowires in AAO.

The lengths of the deposited nanowires were measured by using SEM analysis of longitudinal template cross-sections in the vertical direction. The effect of natural convection on the inhomogeneity of the lengths of nanowires was established. It was shown that a decrease in the deposition overpotential reduces the inhomogeneity of nanowire lengths. The deposition of nanowires occurs more slowly near the top boundary of the templates due to the influence of the cell walls, which leads to additional inhomogeneity.

Simulation of the process of pore filling with metal under natural convection conditions was performed. We developed a model that takes into account the transfer of only the metal cations and their concentration in the electrolyte under the influence of natural convection. The model includes the resulting system of Fick and Navier–Stokes equations in the Boussinesq approximation with boundary conditions describing metal deposition into nanopores, taking into account the deposition kinetics. It is shown that the inhomogeneity of nanowire lengths was qualitatively described by the model system.

An analytical expression has been proposed for the dependence of the deposition current density on time under natural convection conditions. With the help of fitting, the parameters of the deposition kinetics were selected so that the proposed expression agrees well with the corresponding experimental dependencies.

The influence of natural convection can significantly decrease the uniformity of pore filling in different parts of the template, depending both on the location of the template in space or on the conditions of electrolyte stirring in the electrochemical cell (forced convection). The results obtained in this work are not only interesting from a fundamental point of view but can also be used for applications of obtaining homogeneous arrays of nanowires.

CRediT authorship contribution statement

I.A. Kalinin: Investigation, Methodology, Writing – original draft, Validation. **A.D. Davydov:** Conceptualization, Methodology, Writing – review & editing. **A.P. Leontiev:** Resources, Investigation. **K.S. Napolskii:** Conceptualization, Methodology, Writing – review & editing. **A. Sobolev:** Resources, Investigation. **M. Shatalov:** Resources,

Investigation. **M. Zinigrad:** Conceptualization, Methodology, Writing – review & editing. **D. Bograchev:** Conceptualization, Methodology, Writing – original draft.

Declaration of Competing Interest

...The authors declare that they have no known competing financial interests or personal relationships that could have appeared to influence the work reported in this paper.

Data availability

No data was used for the research described in the article.

Acknowledgments

The work was financially supported by Ariel University, Department of Chemical Sciences. IAK, APL, and KSN thank the Russian Science Foundation for the financial support of the present work (Grant No. 18-73-10151).

References

[1] M.T. Borgström, J. Wallentin, M. Heurlin, S. Fält, P. Wickert, J. Leene, M. H. Magnusson, K. Deppert, L. Samuelson, Nanowires with promise for photovoltaics, IEEE J. Sel. Top. Quantum Electron. 17 (2010) 1050–1061.
[2] N.I. Goktas, P. Wilson, A. Ghukasyan, D. Wagner, S. McNamee, R.R. LaPierre, Nanowires for energy: a review, Appl. Phys. Rev. 5 (2018) 41305.
[3] K. Yu, X. Pan, G. Zhang, X. Liao, X. Zhou, M. Yan, L. Xu, L. Mai, Nanowires in energy storage devices: structures, synthesis, and applications, Adv. Energy Mater. 8 (2018), 1802369.
[4] M.P. Proenca, C.T. Sousa, J. Ventura, M. Vazquez, J.P. Araujo, Ni growth inside ordered arrays of alumina nanopores: enhancing the deposition rate, Electrochim. Acta 72 (2012) 215–221, https://doi.org/10.1016/j.electacta.2012.04.036.
[5] K.S. Napolskii, I. v Roslyakov, A.A. Eliseev, D.I. Petukhov, A.V. Lukashin, S.-F. Chen, C.-P. Liu, G.A. Tsirlina, Tuning the microstructure and functional properties of metal nanowire arrays via deposition potential, Electrochim. Acta 56 (2011) 2378–2384, https://doi.org/10.1016/j.electacta.2010.12.013.
[6] A.W. Lodge, M.M. Hasan, P.N. Bartlett, R. Beanland, A.L. Hector, R.J. Kashtiban, W. Levason, G. Reid, J. Sloan, D.C. Smith, Electrodeposition of tin nanowires from a dichloromethane based electrolyte, RSC Adv. 8 (2018) 24013–24020.
[7] F.S. Fedorov, P. Dunne, A. Gebert, M. Uhlemann, Influence of Cu2+ ion concentration on the uniform electrochemical growth of copper nanowires in ordered alumina template, J. Electrochem. Soc. 162 (2015) D568.
[8] D.A. Bograchev, A.D. Davydov, The role of common outer diffusion layer in the metal electrodeposition into template nanopores, Electrochim. Acta 367 (2021), 137405, https://doi.org/10.1016/j.electacta.2020.137405.
[9] D. Bograchev, V. Volgin, A. Davydov, Simple model of mass transfer in template synthesis of metal ordered nanowire arrays, Electrochim. Acta 96 (2013) 1–7, https://doi.org/10.1016/j.electacta.2013.02.079.
[10] L. Philippe, N. Kacem, J. Michler, Electrochemical deposition of metals inside high aspect ratio nanoelectrode array: Analytical current expression and multidimensional kinetic model for cobalt nanostructure synthesis, J. Phys. Chem. C 111 (2007) 5229–5235, https://doi.org/10.1021/jp0677997.
[11] A. Ghahremaninezhad, A. Dolati, Diffusion-controlled growth model for electrodeposited cobalt nanowires in highly ordered aluminum oxide membrane, ECS Trans. (2010) 13–25, https://doi.org/10.1149/1.3503348.
[12] D.A. Bograchev, V.M. Volgin, A.D. Davydov, Modeling of metal electrodeposition in the pores of anodic aluminum oxide, Russ. J. Electrochem. 51 (2015) 799–806, https://doi.org/10.1134/S1023193515090049.
[13] D.A. Bograchev, V.M. Volgin, A.D. Davydov, Simulation of inhomogeneous pores filling in template electrodeposition of ordered metal nanowire arrays, Electrochim. Acta 112 (2013) 279–286, https://doi.org/10.1016/j.electacta.2013.08.171.
[14] A. Fang, M. Haataja, Modeling and analysis of electrodeposition in porous templates, J. Electrochem. Soc. 164 (2017) D875–D887, https://doi.org/10.1149/2.1331713jes.
[15] D.A. Bograchev, A.D. Davydov, Effect of applied temperature gradient on instability of template-assisted metal electrodeposition, Electrochim. Acta 296 (2019) 1049–1054, https://doi.org/10.1016/j.electacta.2018.11.092.
[16] S. Valizadeh, J.M. George, P. Leisner, L. Hultman, Electrochemical deposition of Co nanowire arrays; Quantitative consideration of concentration profiles, Electrochim. Acta 47 (2001) 865–874, https://doi.org/10.1016/S0013-4686(01)00797-6.
[17] M.C. Lopes, C.P. d. Oliveira, E.C. Pereira, Computational modeling of the template-assisted deposition of nanowires, Electrochim. Acta 53 (2008) 4359–4369, https://doi.org/10.1016/j.electacta.2008.01.072.
[18] S. Blanco, R. Vargas, J. Mostany, C. Borras, B.R. Scharifker, C. Borrás, B. R. Scharifker, Modeling the growth of nanowire arrays in porous membrane templates, J. Electrochem. Soc. 161 (2014) E3341–E3347, https://doi.org/10.1149/2.039408jes.
[19] I.U. Schuchert, M.E. Toimil Molares, D. Dobrev, J. Vetter, R. Neumann, M. Martin, Electrochemical copper deposition in etched ion track membranes. Experimental results and a qualitative kinetic model, J. Electrochem. Soc. 150 (2003) C189–C194, https://doi.org/10.1149/1.1554722.
[20] D.L. Zagorskiy, K.V. Frolov, S.A. Bedin, I.V. Perunov, M.A. Chuev, A.A. Lomov, I. M. Doludenko, Structure and Magnetic Properties of Nanowires of Iron Group Metals Produced by Matrix Synthesis, Phys. Solid State 60 (2018) 2115–2126, https://doi.org/10.1134/S1063783418110367.
[21] V.G. Levich, Physicochemical Hydrodynamics, Englewood Cliffs, 1962. N.J. http://books.google.fr/books?id=Y1dMMwEACAAJ.
[22] D.A.. Bograchev, A.D. Davydov, Theoretical study of the effect of electrochemical cell inclination on the limiting diffusion current, Electrochim. Acta 47 (2002) 3277–3285, https://doi.org/10.1016/S0013-4686(02)00245-1.
[23] J.K. Novev, R.G. Compton, Natural convection effects in electrochemical systems, Curr. Opin. Electrochem. 7 (2018) 118–129.
[24] V.M. Volgin, A.D. Davydov, Natural-convective instability of electrochemical systems: a review, Russ. J. Electrochem. 42 (2006) 567–608, https://doi.org/10.1134/S1023193506060012.
[25] Y. Konishi, M. Motoyama, H. Matsushima, Y. Fukunaka, R. Ishii, Y. Ito, Electrodeposition of Cu nanowire arrays with a template, J. Electroanal. Chem. 559 (2003) 149–153.
[26] J.-H. Han, E. Khoo, P. Bai, M.Z. Bazant, Over-limiting current and control of dendritic growth by surface conduction in nanopores, Sci. Rep. 4 (2014) 7056, https://doi.org/10.1038/srep07056.
[27] J. Welty, G.L. Rorrer, D.G. Foster, Fundamentals of Momentum, Heat, and Mass Transfer, Wiley, 2014.
[28] D.A. Bograchev, V.M. Volgin, A.D. Davydov, Determination of mass coefficients of ions in a quantitative analysis of the effect of natural convection on electrochemical processes, Russ. J. Electrochem. 41 (2005) 1197–1204, https://doi.org/10.1007/s11175-005-0202-0.
[29] H. Masuda, K. Fukuda, Ordered metal nanohole arrays made by a two-step replication of honeycomb structures of anodic alumina, Science 268 (1995) (1979) 1466–1468, https://doi.org/10.1126/SCIENCE.268.5216.1466.
[30] C.A. Schneider, W.S. Rasband, K.W. Eliceiri, NIH image to ImageJ: 25 years of image analysis, Nat. Methods (2012), https://doi.org/10.1038/nmeth.2089.
[31] L.A. Reznikova, E.E. Morgunova, D.A. Bograchev, A.P. Grigin, A.D. Davydov, Limiting current in iodine-iodide system on vertical electrode under conditions of natural convection, Russ. J. Electrochem. 37 (2001) 382–387.
[32] W. Xing, M. Yin, Q. Lv, Y. Hu, C. Liu, J. Zhang, Oxygen solubility, diffusion coefficient, and solution viscosity, rotating electrode methods and oxygen reduction electrocatalysts. (2014) 1–31. 10.1016/B978-0-444-63278-4.00001-X.
[33] N.D. Nikolić, K.I. Popov, L.J. Pavlović, M.G. Pavlović, The effect of hydrogen codeposition on the morphology of copper electrodeposits. I. the concept of effective overpotential, J. Electroanal. Chem. 588 (2006) 88–98, https://doi.org/10.1016/j.jelechem.2005.12.006.
[34] A.J. Bard, L.R. Faulkner, Electrochemical methods: fundamentals and applications, 1980.
[35] A.M. Sukhotin, *Spravochnik po electrokhimii* (in Russian), Khimia, Leningrad, 1981.
[36] T.I. Quickenden, X. Jiang, The diffusion coefficient of copper sulphate in aqueous solution, Electrochim. Acta 29 (1984) 693–700.
[37] F.H. Bark, Instability during electrodeposition, 40 (1995) 599–614.
[38] C. Chen, J. Jorne, The dynamics of morphological instability during electrodeposition, J. Electrochem. Soc. 138 (1991) 3305–3311, https://doi.org/10.1149/1.2085407.
[39] L.-G. Sundström, F.H. Bark, On morphological instability during electrodeposition with a stagnant binary electrolyte, Electrochim. Acta 40 (1995) 599–614.
[40] V.M. Volgin, O.V. Volgina, D.A. Bograchev, A.D. Davydov, Simulation of ion transfer under conditions of natural convection by the finite difference method, J. Electroanal. Chem. 546 (2003) 15–22.